Journal of Orthopaedic Translation (2019) 16, 40—52

Available online at www.sciencedirect.com

ScienceDirect

journal homepage: http://ees.elsevier.com/jot

ORIGINAL ARTICLE

Articular cartilage regeneration using acellular bioactive affinity-binding alginate hydrogel: A 6-month study in a mini-pig model of osteochondral defects

Emil Ruvinov [a,*], Tali Tavor Re'em [a,☆], Frank Witte [b], Smadar Cohen [a,c,d]

[a] *Avram and Stella Goldstein-Goren Department of Biotechnology Engineering, Ben-Gurion University of the Negev, Beer Sheva, Israel*
[b] *Julius Wolff Institute and Center for Musculoskeletal Surgery, Berlin-Brandenburg Center for Regenerative Therapies, Charité - Universitätsmedizin Berlin, Berlin, Germany*
[c] *Regenerative Medicine and Stem Cell (RMSC) Research Center, Ben-Gurion University of the Negev, Beer Sheva, Israel*
[d] *The Ilse Katz Institute for Nanoscale Science and Technology, Ben-Gurion University of the Negev, Beer Sheva, Israel*

Received 31 May 2018; received in revised form 8 August 2018; accepted 15 August 2018
Available online 9 September 2018

KEYWORDS
Affinity-binding alginate;
Bone morphogenic protein 4;
Hyaline cartilage;
Osteochondral defect;
Transforming growth factor-β1

Abstract *Background:* Despite intensive research, regeneration of articular cartilage largely remains an unresolved medical concern as the clinically available modalities still suffer from long-term inconsistent data, relatively high failure rates and high prices of more promising approaches, such as cell therapy. In the present study, we aimed to evaluate the feasibility and long-term efficacy of a bilayered injectable acellular affinity-binding alginate hydrogel in a large animal model of osteochondral defects.
Methods: The affinity-binding alginate hydrogel is designed for presentation and slow release of chondrogenic and osteogenic inducers (transforming growth factor-β1 and bone morphogenic protein 4, respectively) in two distinct and separate hydrogel layers. The hydrogel was injected into the osteochondral defects created in the femoral medial condyle in mini-pigs, and various outcomes were evaluated after 6 months.
Results: Macroscopical and histological assessment of the defects treated with growth factor affinity-bound hydrogel showed effective reconstruction of articular cartilage layer, with major features of hyaline tissue, such as a glossy surface and cellular organisation, associated with marked deposition of proteoglycans and type II collagen. Microcomputed tomography

* Corresponding author. Ben-Gurion University of the Negev, POB 653, Beer Sheva, 84105, Israel.
E-mail address: ruvinove@bgu.ac.il (E. Ruvinov).
☆ Current address: Department of Pharmaceutical Engineering, Azrieli College of Engineering, Jerusalem, Israel.

https://doi.org/10.1016/j.jot.2018.08.003

showed incomplete bone formation in both treatment groups, which was nevertheless augmented by the presence of affinity-bound growth factors. Importantly, the physical nature of the applied hydrogel ensured its shear resistance, seamless integration and topographical matching to the surroundings and opposing articulating surface.
Conclusions: The treatment with acellular injectable growth factor—loaded affinity-binding alginate hydrogel resulted in effective tissue restoration with major hallmarks of hyaline cartilage, shown in large animal model after 6-month follow-up.
The translational potential of this article: This proof-of-concept study in a clinically relevant large animal model showed promising potential of an injectable acellular growth factor—loaded affinity-binding alginate hydrogel for effective repair and regeneration of articular hyaline cartilage, representing a strong candidate for future clinical development.

Introduction

Regeneration of articular cartilage remains an unmet medical need, which imposes a heavy burden on global economy and on the health-care community. Articular cartilage defects mainly (60—80% of cases) result from mechanical trauma (e.g., sport injuries) [1]. Patients with acute traumatic injuries of the joint have a higher chance of developing posttraumatic osteoarthritis, a degenerative condition that results in severe pain and disability, eventually requiring a total knee replacement [2].

Regardless of aetiology, articular cartilage defects are typically irreversible due to the unique features of hyaline cartilage, such as its avascular nature, and consequent lack of access to a pool of potential reparative cells or humoural factors. In osteochondral defects, which have access to the mesenchymal stem cells of the bone marrow, the uncontrolled repair response typically leads to the formation of functionally inferior fibrocartilage [3]. This type of repair is generally encountered after microfracture (MF), a surgical marrow stimulation technique, which is considered as a first-line treatment for articular cartilage defects [recommended for small (<2—3 cm) defects] and usually results in inconsistent and poor long-term outcomes [4]. Osteochondral autograft transplantation (recommended for 2- to 3-cm, as well as for larger defects), although suggested to result in better outcomes, is associated with donor site morbidity and the lack of integration and surface restoration due to the solid nature of the implant [5]. Autologous cartilage implantation (ACI) and matrix-assisted ACI developed more recently (recommended for defects larger than 3 cm) show promising clinical results, but some major drawbacks of these therapies include relatively high failure rates, the need for two separate surgeries and cell processing and high prices [5]. In a 14- to 15-year follow-up study, ~50% of patients in both ACI and MF groups developed radiological signs of early osteoarthritis [6].

Clinical experience clearly shows that the effective treatment that results in regeneration of durable hyaline cartilage is yet to be found. A variety of tissue engineering strategies is being developed, aimed to achieve this goal. These include stem cell—based therapies, implantation of hydrogels or solid scaffolds and combinations with growth factors [5]. In the previous work, Freeman et al and Ruvinov et al developed a bio-inspired affinity-binding alginate biomaterial consisting of an alginate—sulphate/alginate combination, in which various heparin-binding growth factors can be bound to alginate—sulphate with high affinity, effectively mimicking their natural interaction with heparin/heparan sulphate glycosaminoglycans in the extracellular matrix (ECM) [7,8]. This acellular and injectable platform was successfully tested *in vivo* in various disease models, including myocardial infarction, hind limb ischaemia, and spinal cord injury [8—11]. For osteochondral defect repair, a platform consisting of chondroinductive transforming growth factor-β1 (TGF-β1) and the osteoinductive bone morphogenic protein 4 (BMP-4) presented spatially in two distinct hydrogel layers. The feasibility of the bilayer strategy to induce simultaneous regeneration of articular cartilage and subchondral bone in osteochondral defects has been demonstrated in rabbits with follow-up period of 4 weeks [12].

In the present study, we aimed to test the feasibility and long-term efficacy of bilayered application of TGF-β1/BMP-4—affinity-binding alginate hydrogel in a clinically relevant model of osteochondral defects in mini-pigs. Mini-pigs are frequently used as a large animal model for articular cartilage and subchondral bone repair due to the structural and weight-bearing similarities to humans, and this is one of the recommended models for preclinical development of cartilage repair products by the US Food and Drug Administration [13,14]. To the best of our knowledge, this is the first report evaluating acellular and injectable growth factor—biomaterial combination therapy for the treatment of articular cartilage defects with 6-month follow-up in a large animal model.

Materials and methods

Materials and animals

Sodium alginate (VLVG, >65% guluronic acid monomer content) was purchased from FMC Biopolymers (Drammen, Norway). Alginate sulphate was synthesised from sodium alginate (VLVG) as previously described [7]. Human

recombinant TGF-β1 and BMP-4 were purchased from Peprotech (Rocky Hill, NJ). All chemicals, unless specified otherwise, were from Sigma–Aldrich, and were of analytical grade.

Three adult, skeletally mature [13,14] Sinclair mini-pigs (males, 13-month old, ~40 kg) were acquired from Harlan laboratories (Jerusalem, Israel). The experiments were conducted in Lahav CRO (Kibbutz Lahav, Israel) facility under an ethical committee–approved protocol (IL-12-09-156) in accordance with local legislation and guidelines.

Preparation of injectable growth factor–loaded affinity-binding alginate hydrogel

The growth factor–alginate sulphate bioconjugates were prepared by mixing and incubation of TGF-β1 or BMP-4 solutions (reconstituted according to manufacturer's instructions to a concentration of 500 μg/ml) with alginate sulphate solution (3%, w/v) for 1 h at 37°C to allow equilibrium binding of the factor. Stock solutions of sodium alginate (VLVG) and D-gluconic acid/hemicalcium salt were prepared by dissolving the materials in double-distilled water (DDW) and stirring at room temperature. Each solution was filtered separately through a sterile 0.2-μm filter membrane into a sterile container in a laminar flow cabinet. Equal volumes from each stock solution [5.3% and 3% (w/v) for VLVG alginate and D-gluconic acid, respectively] were combined by extensive homogenisation for several minutes to facilitate homogenous distribution of the calcium ions and cross-linking of alginate chains. Finally, the TGF-β1 and BMP-4/alginate sulphate bioconjugates were mixed with the cross-linked alginate solution to yield injectable, affinity-bound TGF-β1 or BMP-4-alginate solutions with the following compositions: i) TGF-β1–containing (cartilage forming) layer—0.67% alginate sulphate, 1.82% alginate, 1.03% D-gluconic acid, all w/v, and 44.4 μg/mL of protein; ii) BMP-4–containing (bone forming) layer—0.87% alginate sulphate, 1.78% alginate, 1.0% D-gluconic acid, all w/v, and 18.7 μg/mL of protein. For the documentation of hydrogel application procedure and layer formation, 10 μL of methylene blue solution (10 mg/mL in DDW) was added to the bottom layer hydrogel.

Osteochondral defect model in Sinclair mini-pigs and hydrogel application

Using general anaesthesia and a sterile technique, an anteromedial mini-arthrotomy of ~3 cm was performed, and the patella was laterally dislocated. Standard osteochondral autograft transfer system (OATS) core punch (Arthrex, Naples, FL) was used to create an osteochondral defect (6 mm in diameter and 8 mm deep) in the weight-bearing zone of the medial femoral condyle.

The defect was cleaned and rinsed with sterile saline and then washed with calcium chloride solution. The defect was first filled with BMP-4/affinity-binding alginate hydrogel up to the cartilage layer, and in situ gelation was induced by the addition of 1 M $CaCl_2$. After gelation of the bottom layer (5 min), the top layer of the TGF-β1/affinity-binding alginate was similarly constructed. The amount of loaded TGF-β1 or BMP-4 in each layer was ~10 μg (44.4 μg/mL and 18.7 μg/mL for TGF-β1 and BMP-4, respectively). This dose was chosen based on rough extrapolation of the protein amount used previously in rabbits (300–400 ng) using fold-increase in animal weight (from rabbits to mini-pigs). Contralateral knees were treated with empty [w/o growth factors (GFs)] affinity-binding alginate hydrogel. The condyle was gently repositioned correctly under the meniscus, and the knee was extended fully and then bent several times to reshape the surface of the hydrogel to local anatomy. The complete retention of both hydrogel layers in the defect was confirmed before final closure. Hoffa's fat pad, subcutaneous layer and skin were then sutured. X-ray in two planes for each distal femur was performed to document the operation site and defect orientation and confirm the lack of fractures. The animals were then returned to their cages and allowed to move freely with full load bearing and no external support.

Intravital polychromatic staining for the evaluation of subchondral bone formation

To evaluate time-resolved bone formation, an injection series of two fluorochromes was applied [15,16]. Calcein green (2% solution in 2% sodium bicarbonate, all w/v) was administered intravenously by slow bolus injection on Day 10 and 20 after operation, at 20 mg/kg body weight. On days 20 and 10 before euthanasia/explantation, xylenol orange (Waldeck, Munster, Germany) (9% solution in 2% sodium bicarbonate, all w/v) was administered intravenously at 90 mg/kg body weight by slow bolus injection.

Animal euthanasia, gross morphology and sample explantation

The mini-pigs were euthanised 6 months after operation by administration of an overdose of 3% sodium pentobarbital. The knee joints were opened, and the macroscopic appearance and the quality of the filling was evaluated using International Cartilage Research Society (ICRS) macroscopic evaluation score (Table 1) [17]. The defects were then explanted using 15-mm OATS core punch, snap-frozen in liquid nitrogen and stored at −80°C until further analyses.

Microcomputed tomography (μCT)

The frozen explants were scanned using a specially constructed microtomography device at the Technische Universitat Dortmund, Germany. The main components of the microtomograph are a microfocus X-ray tube (Scanray, Germany) with a focal spot <10 μm and maximum acceleration voltage of 150 kV, a four-axis precision sample manipulator and a 2D radiation image detector (RID 512-400, active area of 204.8 × 204.8 mm; Perkin Elmer, Waltham, MA, USA) [18].

The extent of bone formation was quantified using 2D μCT images in two planes parallel to Z axis (ZX and ZY) by measurement of the percentage of area filled with bone in the region of interest of original defect size (6 × 8 mm, calibrated using image scale bar) placed over the defect.

Table 1 ICRS macroscopic evaluation score.

Characteristic	Grading	Score
Degree of defect repair	Level of surrounding cartilage	4
	75% repair of defect depth	3
	50% repair	2
	25% repair	1
	0% repair	0
Integration to border zone	Complete integration with border zone	4
	Demarcating border <1 mm	3
	3/4 of repair tissue integrated, 1/4 with notable border >1 mm	2
	1/2 of repair integrated with surrounding cartilage, 1/2 with a notable border >1 mm	1
	From no contact to 1/4 of repair integrated with surrounding cartilage	0
Macroscopic appearance	Intact smooth surface	4
	Fibrillated surface	3
	Small, scattered fissures or cracks	2
	Several, small or few but large fissures	1
	Total degeneration of defect area	0
Total, max		**12**

ICRS, International Cartilage Research Society.

All measurements were performed using ImageJ software, version 1.51k (National Institutes of Health, https://imagej.nih.gov/ij/).

Histology and immunohistochemistry

Explants were fixed in 4% paraformaldehyde (v/v, in Phosphate-buffered saline (PBS), pH 7.4) for 7 d. After embedding and polymerisation in methyl methacrylate (Technovit 9100 Newl, Heraeus-Kulzer, Hanau, Germany), thin sections (5-μm thick) were cut using an RM 2155 microtome (Leica, Bensheim, Germany). Before staining, sections were deacrylated in xylol (2 × 15 min) and 2-methoxyethylacetate (2 × 10 min), cleared in a decreasing ethanol series (2 × isopropyl alcohol, 2 × 96% ethanol, 2 × 70% ethanol, 2 min each) and rehydrated in distilled water. Rehydrated sections were incubated in 0.1% Toluidine blue or Safranin O for 20 s, washed in distilled water, dehydrated in ethanol and mounted in Eukitt (Labonord, Monchengladbach, Germany). Sections near the center of the defect were assessed for tissue quality and structural and cellular changes using modified O'Driscoll semiquantitative scoring system (Table 2) [19].

Polychromatic staining for the evaluation of time-resolved bone formation (calcein green and xylenol orange) was visualised using Olympus light microscope (BX61, Motorized System Microscope, Tokyo, Japan) equipped with appropriate sets of fluorescence filters, connected to an Olympus digital capture system (DP71) and Olympus Cell^P software.

For type II collagen immunohistochemistry, the rehydrated sections were first mildly digested for antigen retrieval with 2% (v/v) proteinase K (Dako, Glostrup, Denmark) in Tris-buffered saline (TBS) for 20 min at 37°C, followed by a short wash in TBS and a decalcification step in EDTA buffer for 60 min at 37°C. After washing in TBS, sections were preincubated with a solution of 3% (v/v) H_2O_2 in TBS for 30 min to block endogenous peroxidase activity, followed by an incubation for 30 min in a solution of 10% (v/v) normal goat serum (Vector/Linaris, Wertheim-Bettingen, Germany) in TBS to block unspecific binding. The primary rabbit anti-collagen II antibody (1:200 dilution) (ab34712, Abcam, Cambridge, UK) was applied for 60 min at room temperature. The sections were washed three times in TBS (5 min each), followed by reacting with peroxidase-labelled secondary antibody for 30 min at room temperature. Peroxidase activity is visualised using the liquid DAB (3,3′-diaminobenzidine) substrate chromogen system (Dako). Sections were then washed twice with TBS and distilled water and finally mounted with Aquatex (Merck, Darmstadt, Germany). Photomicrographs were taken with a Zeiss Axioskop 40 microscope equipped with a Zeiss AxioCam Mrc digital camera and Zeiss AxioVision software (Zeiss, Oberkochen, Germany) or Olympus light microscope (BX61, Motorized System Microscope) connected to an Olympus digital capture system (DP71) and Olympus Cell^P software (Olympus, Tokyo, Japan).

Statistical analysis

Statistical analysis was performed with GraphPad Prism version 7.03 for Windows (GraphPad Software, San Diego, CA). All variables were expressed as mean ± standard deviation. Histological scores and bone filling between treatment groups were compared using Mann–Whitney test. A p value < 0.05 was considered statistically significant.

Results

Osteochondral defect model in mini-pigs

The mini-pig study design is shown in Fig. 1A. Osteochondral defects (Fig. 1B) were created in the weight-bearing region of the medial femoral condyle using a commercially available OATS core punch that allows reproducible defect creation with controlled diameter and depth. The correct orientation of the defects and the lack of bone fractures were confirmed by X-ray imaging (Supplementary Fig. S1). Initial bleeding was detected in the defects as expected due to perforation of subchondral bone to the desired defect depth (~6 mm). After the surgery and the recovery from anaesthesia, all animals were mobile and could move freely. The lameness of the animals gradually improved and was not evident 10 days after operation. During the 6-month follow-up period, there was no evidence of any restriction of movement or any other adverse effects of the treatment.

Table 2 Modified O'Driscoll histological score.

Characteristic	Grading	Score
I. Nature of predominant tissue	Hyaline cartilage	4
	Mostly hyaline cartilage	3
	Mixed hyaline and fibrocartilage	2
	Mostly fibrocartilage	1
	Some fibrocartilage, mostly nonchnodrocytic cells	0
II. Structural characteristics		
A. Surface irregularity	Smooth and intact	3
	Superficial horizontal lamination	2
	Fissures	1
	Severe disruption, including fibrillation	0
B. Structural integrity, homogeneity	Normal	2
	Slight disruption, including cysts	1
	Severe disintegration, disruptions	0
C. Thickness	100% of normal adjacent cartilage	2
	50—100% or thicker than normal	1
	0—50% of normal cartilage	0
D. Bonding to adjacent cartilage	Bonded at both ends of graft	2
	Bonded at one end or partially both ends	1
	Not bonded	0
III. Freedom from cellular changes of degeneration		
A. Hypocellularity	Normal cellularity	2
	Slight hypocellularity	1
	Moderate hypocellularity, or hypercellularity	0
B. Chondrocyte clustering	No clusters	2
	<25% of the cells	1
	25—100% of the cells	0
IV. Freedom from degenerate changes in adjacent cartilage	Normal cellularity, no clusters, normal staining	3
	Normal cellularity, mild clusters, moderate staining	2
	Mild or moderate hypo/hypercellularity, slight staining	1
	Severe hypocellularity, poor or no staining	0
V. Subchondral bone		
A. Reconstruction of subchondral bone	Normal	3
	Reduced subchondral bone reconstruction	2
	Minimal subchondral bone reconstruction	1
	No subchondral bone reconstruction	0
B. Inflammatory response in subchondral bone region	None/mild	2
	Moderate	1
	Severe	0
VI. Safranin O staining	Normal or near normal	3
	Moderate	2
	Slight	1
	None	0
Total, max		**28**

Physical properties of the hydrogel

The hydrogel consisted of a mixture of calcium cross-linked solution of alginate [1.82% w/v of 30 kDa VLVG alginate and 1.03% (w/v) D-gluconic acid/hemicalcium salt] and the bioconjugate of growth factor—alginate sulphate (0.67% w/v). At preparation, the biomaterial displayed low apparent viscosity of 5—7 Pa*s at a shear rate of 10 s^{-1}, and its mechanical spectrum revealed storage (G') and loss (G'') moduli values that are closely related (60 Pa) and shared a cross-point at low frequency, according to rheology. This type of physical behaviour usually characterises cross-linked material on the verge of phase transition from the liquid state into a hydrogel. After administration into the osteochondral defect, the transition to solid hydrogel occurred with the addition of calcium chloride solution, which further cross-links the alginate chains, yielding a matrix with an elastic modulus of 2 kPa (100 times greater), a value close to that measured for extracellular matrix (ECM) [20].

Hydrogel application

After the bleeding was stopped, the defect "bed" was prepared by brief washing with sterile calcium chloride solution, and the hydrogel layers were applied immediately

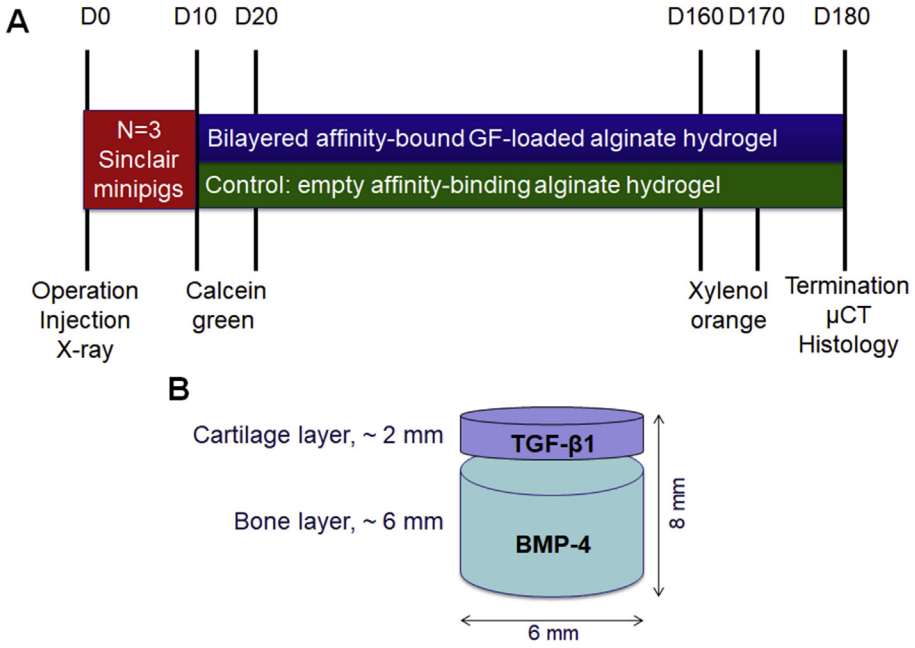

Figure 1 (A) Mini-pig study design and (B) schematic illustration of defect dimensions and respective hydrogel layers applied.

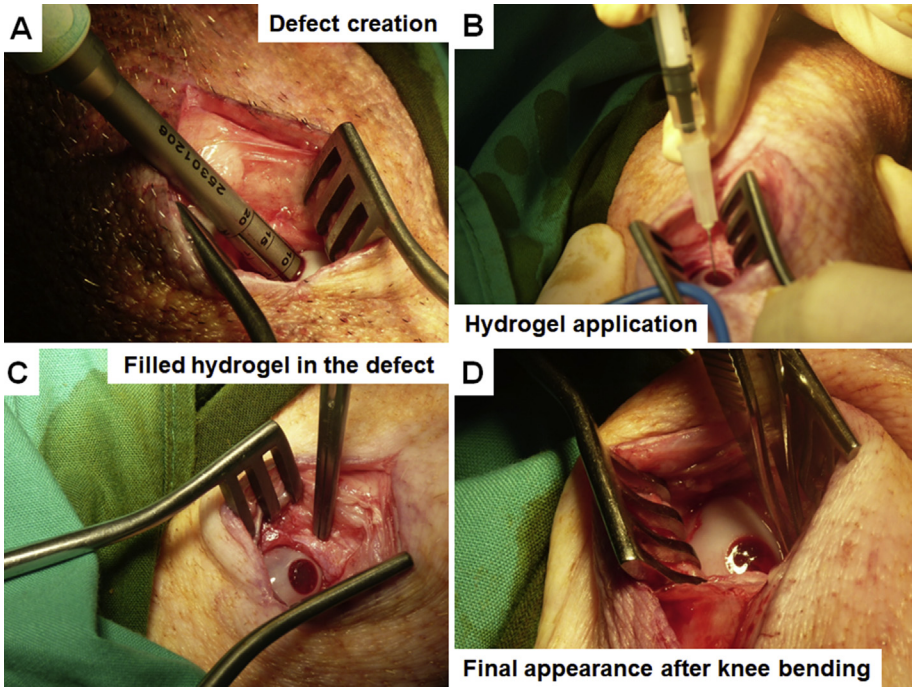

Figure 2 Hydrogel application procedure. (A) Defect creation using 6-mm OATS core punch in the medial femoral condyle. The depth of the defect was monitored using the depth laser marks. (B) Injection of the hydrogel. First, bottom layer (BMP-4-containing) was applied, followed by *in situ* gelation by cross-linking using calcium chloride, then top (TGFβ1-containing) layer was applied and gelated similarly. (C) The appearance of the gelated bilayered hydrogel in the defect after application. (D) Final appearance of the hydrogel in the defect after several rounds of knee bending and full limb extension. Note complete material retention in the defect and reshaping of the surface matching local topography.
BMP-4 = bone morphogenic protein 4; OATS = osteochondral autograft transfer system; TGFβ1 = transforming growth factor-β1.

after. Overall hydrogel application procedure is shown in Fig. 2 and Supplementary Movie 1. First, bottom, BMP-4-affinity-bound alginate hydrogel layer was applied by simple injection, followed by fast (several minutes) gelation induced by the addition of calcium chloride cross-linker. The semi-solid nature of the hydrogel in the defect allows easy reshaping and modulation of the surface (topography, height) to match the specific requirements of any real-life

defect (Supplementary Fig. S2). After the formation of the subchondral gel layer, the top, TGFβ1-affinity-bound alginate hydrogel layer was applied and cross-linked in a similar fashion. Importantly, at any step, the hydrogel may be easily removed from the defect, and the application procedure can be repeated in a matter of minutes.

Supplementary video related to this article can be found at https://doi.org/10.1016/j.jot.2018.08.003.

The final step of the bilayered hydrogel application included relocation of the condyle under the meniscus and performance of several rounds of knee bending (from fully extended limb to maximally flexed position) (Supplementary Fig. S3). This procedure aimed to test the retention of the hydrogel layers in the defect while simultaneously reshaping the hydrogel surface to adapt to local condyle—meniscus interface and complex curvature. This bending test showed complete retention, mechanical stability and shear-resistance of both hydrogel layers in the defect, concomitantly with surface adaptation.

μCT and subchondral bone repair

μCT evaluation of the defects 6 months after operation/treatment showed incomplete filling of subchondral bone in both treatment groups (Fig. 3A). Nevertheless, the treatment with GF-affinity-bound bilayered alginate hydrogel (containing affinity-bound BMP-4 in the bottom, subchondral layer of the defect) was associated with a trend towards higher degree of subchondral bone regeneration and defect closure, shown by an increase in the bone-occupied fractional area, compared with the empty bilayered hydrogel (31.0 ± 6.7% vs. 16.2 ± 6.1%, p = 0.25, and 25.1 ± 4.4% vs. 15.1 ± 0.5%, p = 0.1, in ZX and ZY planes, respectively) (Fig. 3B). Importantly, no abnormal bone formation or bone penetration into the cartilage layer was observed in both treatment groups.

To evaluate time-resolved subchondral bone formation, a series of fluorochrome injections were applied during the study follow-up (Fig. 4). Microscopical evaluation of dye fluorescence showed that the treatment with GF-affinity-bound bilayered alginate hydrogel was associated with more advanced front and continuous bone formation (last 10—20 days of the study), shown by the presence of xylenol orange (administered before euthanasia) signal distantly from calcein green (administered after operation/treatment).

Macroscopic evaluation of cartilage repair

Six months after operation, gross morphological evaluation of the defects revealed regenerated tissue of high quality in the defects treated with GF-affinity-bound (with affinity-

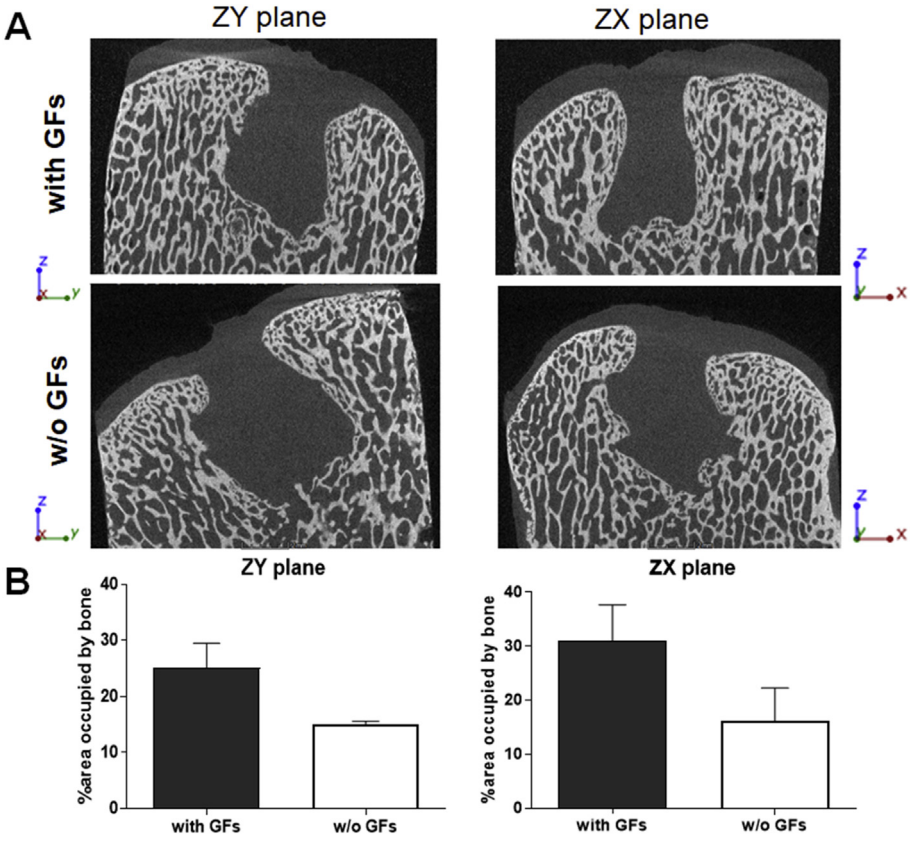

Figure 3 μCT evaluation of subchondral bone formation, 6 months after operation/treatment. (**A**) Representative scans of the defects in the two treatment groups in two planes parallel to the Z axis (ZY and ZX). (**B**) Quantification of the area percentage (from the original defect) filled with newly formed bone.
μCT = microcomputed tomography.

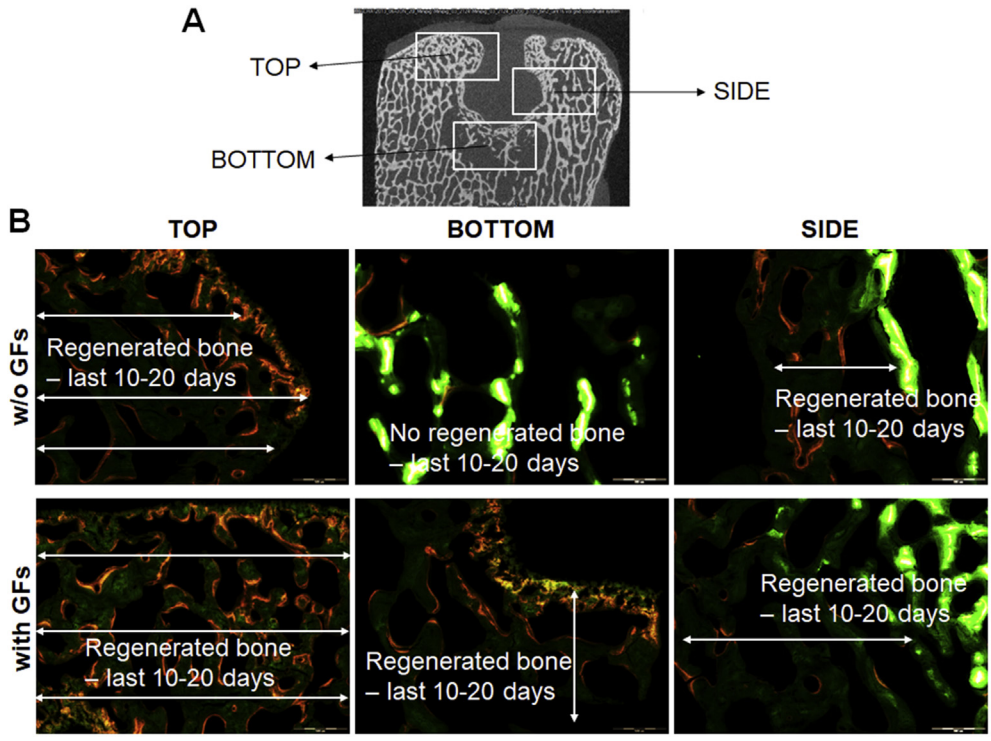

Figure 4 Microscopic evaluation of bone formation at 6 months after operation/treatment, detected by calcein green (administered IV on days 10 and 20 after operation/treatment) and xylenol orange (administered IV on days 20 and 10 before euthanasia/explantation). (**A**) Location map of areas shown in (**B**). (**B**) Representative photomicrographs showing bone formation in each treatment group at various defect locations. The presence of a more advanced front of bone formation (identified by the presence of xylenol orange distantly from calcein green) is evident in the defect treated with affinity-bound GF-loaded alginate hydrogel. Intense green, calcein green; orange-red, xylenol orange. Bar = 500 μm.

bound TGFβ1 in the top layer) bilayered alginate hydrogel (Fig. 5 and Supplementary Movie 2). This treatment resulted in defect filling with glossy and smooth tissue closely resembling the surrounding healthy articular cartilage, associated with good integration with defect surroundings and the lack of clear defect borders. The treatment with empty (w/o GFs) bilayered hydrogel resulted in good defect filling but was associated with inferior tissue morphology. The ICRS macroscopic assessment score was significantly higher in the group treated with the GF-affinity-bound bilayered alginate hydrogel than in the group treated with the empty bilayered hydrogel (10.3 ± 2.9 vs. 5.3 ± 0.6, $p = 0.04$) (Fig. 6A).

Supplementary video related to this article can be found at https://doi.org/10.1016/j.jot.2018.08.003.

Histological assessment of cartilage repair

Histological evaluation of the defects 6 months after the operation/treatment showed hyaline-like tissue formation in the defects treated with GF-affinity-bound bilayered alginate hydrogel (containing TGFβ1 in the top hydrogel layer) compared with empty bilayered hydrogel. Semi-quantitative assessment of the repair quality in the histological sections was performed using modified O'Driscoll histological scoring system across multiple parameters evaluating both regenerated as well as surrounding tissues. The treatment with GF-affinity-bound bilayered alginate hydrogel resulted in significantly higher overall scores than for the defects treated with empty hydrogel (23.7 ± 2.5 vs. 13.3 ± 1.5, $p = 0.04$) (Fig. 6B).

Toluidine blue (Fig. 7A) and Safranin O (Supplementary Fig. S4A) staining showed a formation of a continuous cartilage layer in the defects treated with GF-affinity-bound bilayered alginate hydrogel, with homogenous stain intensities similar between the defect and its surroundings. Chondrocyte morphology and cell density associated with proteoglycan deposition were also similar between the defect and healthy surrounding cartilage, although some lack of columnar organisation was evident (Fig. 7B, and Supplementary Fig. S4B and S5).

In contrast, the treatment with the empty bilayered hydrogel resulted in the marked gap in the stain distribution in the defect center, with stain inhomogeneity throughout the defect. The defect tissue lacked normal organisation and was filled mainly by disorganised hypertrophied tissue and fibrocartilage.

Immunostaining for type II collagen confirmed the histological findings (Fig. 8). The treatment with GF-affinity-bound bilayered alginate hydrogel showed a similar staining pattern and intensity of collagen type II–rich cartilaginous ECM between the defect zone and the surrounding cartilage. In contrast, the treatment with empty bilayered hydrogel resulted in disorganised staining pattern with regions of faint type II collagen staining compared to defect surroundings.

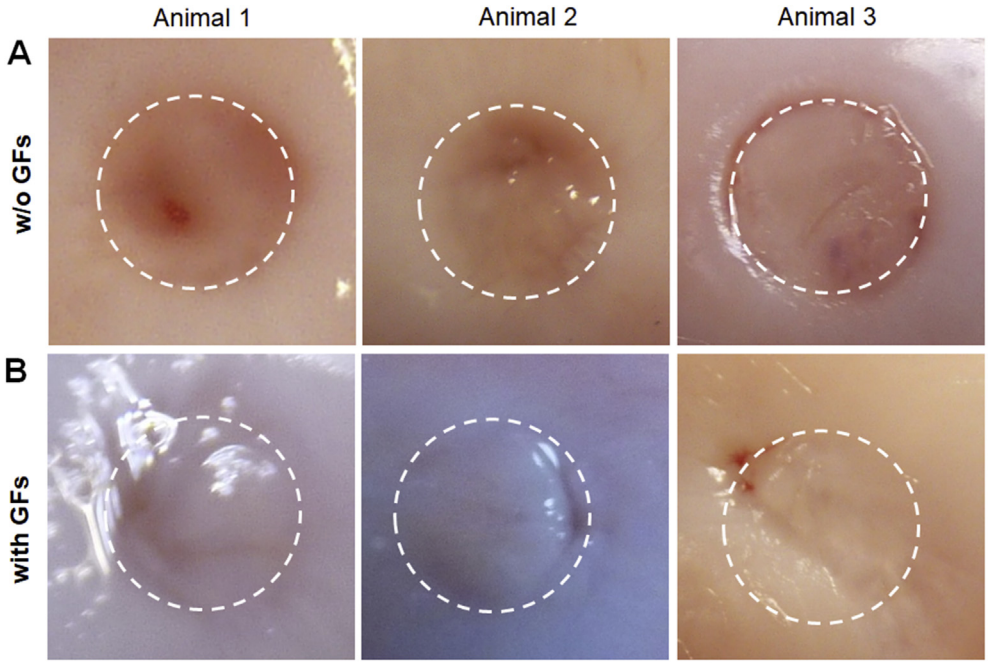

Figure 5 Articular cartilage regeneration 6 months after the treatment with TGFβ1/BMP-4-affinity-bound bilayered alginate hydrogel. Macroscopic appearance of the defects after (**A**) treatment with GF-loaded hydrogel or (**B**) after the treatment with empty hydrogel. Dotted circle represents defect borders. Note similarity in tissue appearance to surrounding cartilage in the defects treated with affinity-bound GF-loaded alginate hydrogel.
BMP-4 = bone morphogenic protein 4; TGFβ1 = transforming growth factor-β1.

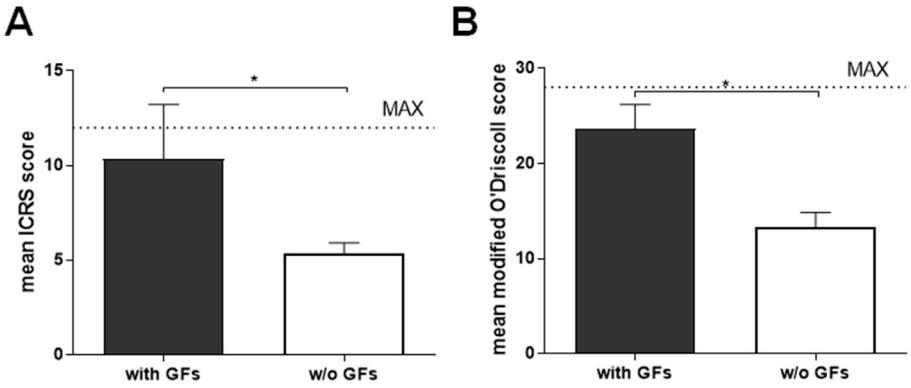

Figure 6 ICRS macroscopic (**A**) and microscopic modified O'Driscoll (**B**) scores of the defects at 6 months after operation/treatment. *<0.05 (Mann—Whitney test). Maximal scores in ICRS and modified O'Driscoll systems are 12 and 28, respectively (shown by dotted line). ICRS, International Cartilage Research Society.

Both treatments showed no signs of degenerative changes in adjacent cartilage and no inflammatory response.

Discussion

In this proof-of-concept study, we showed that treatment with acellular injectable TGFβ1/BMP-4-affinity-bound bilayered alginate hydrogel resulted in effective regeneration of the articular surface, with major structural properties of hyaline cartilage. These results were achieved after a long-term (6 months) follow-up in a clinically relevant large animal model of osteochondral defects.

Multiple tissue engineering strategies are being developed, aimed at regeneration of hyaline cartilage, and several of them are already at various stages of clinical development [5]. Stem cell—based therapies, although holding a great promise, still face several hurdles, such as heterogeneity in cell populations, need for cell processing, lengthy regulatory path and associated costs [21]. Thus, acellular strategies, in which biomaterials can be effectively combined with key signaling/differentiation factors, that can induce and direct endogenous regeneration in situ serve as a valid alternative for clinical translation. Affinity-binding alginate, prepared from algae-derived polysaccharide without the use of animal-derived components,

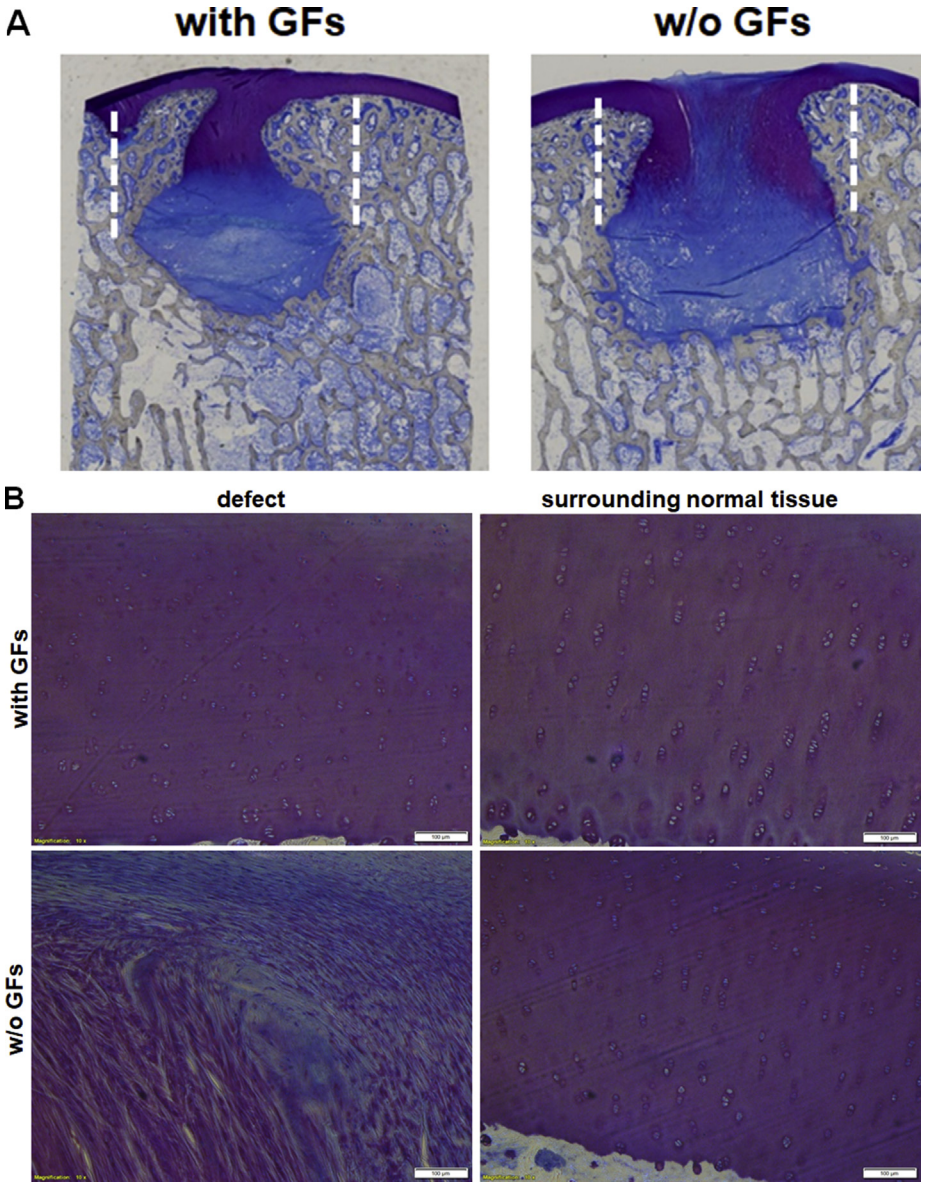

Figure 7 Toluidine blue staining of the treated defects at 6 months after operation/treatment. (**A**) Low-power magnification of representative photomicrographs of the two treatment groups. The treatment with affinity-bound GF-loaded alginate hydrogel resulted in formation of a continuous cartilage layer. (**B**) High-power magnification of the defect and distant surrounding tissue in each treatment group. The treatment with affinity-bound GF-loaded alginate hydrogel resulted in similar stain intensity and morphological similarity to normal hyaline cartilage, although mostly lacking columnar organisation. In contrast, the treatment with empty hydrogel resulted in marked differences in stain intensity and cellular organisation, mainly showing disorganised hypertrophic tissue and fibrocartilage. Bar = 100 μm. Dotted lines represent original defect borders.
GF = growth factor.

represents such an acellular and biocompatible platform where multiple growth factors can be spatially presented via affinity binding in a bio-inspired manner, which was shown previously to maintain their prolonged delivery and presentation in several disease models *in vivo* [8,9,11,12]. Importantly, the biomaterial platform applied herein present additional benefits due to its physical properties. When administered to the osteochondral defect, the biomaterial flows and can completely fill the defect, even if the defect is inconsistent. Later, with the additional cross-linking, the resultant hydrogel resembles ECM, according to elastic modulus.

The osteochondral defect model in the mini-pigs is widely used for cartilage repair studies due to structural similarities to human cartilage and lack of spontaneous regeneration, and it is one of the recommended models for preclinical development of articular cartilage repair products [13,14]. The long-term effects and the potential of the treatment to induce durable cartilage regeneration in large animal models could be, however, fully realised only after a 6-month period [13,14]. Our 6-month mini-pig study shows that the administration of TGFβ1/BMP-4-affinity-binding bilayered alginate hydrogel resulted in reconstruction of continuous articular cartilage layer. This was associated

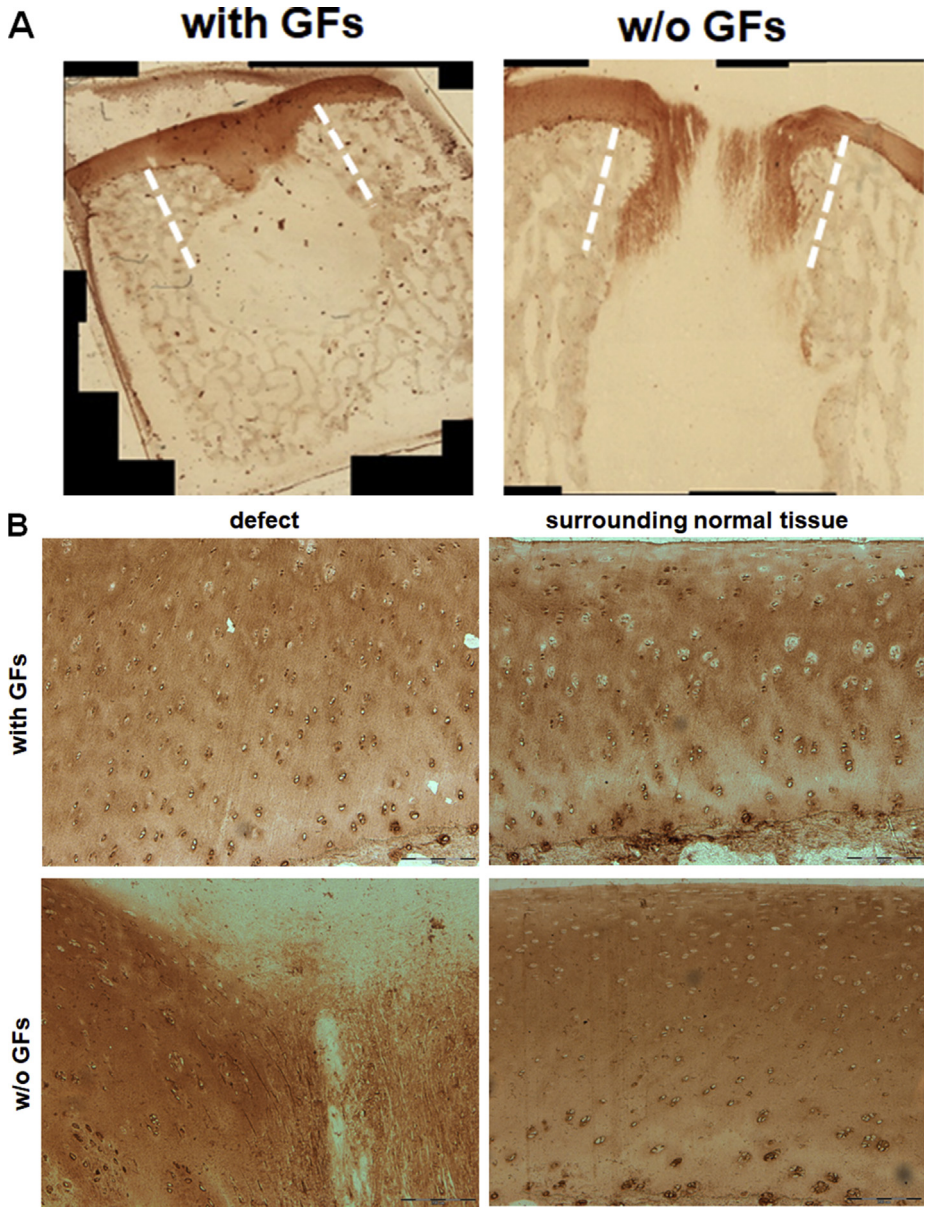

Figure 8 Type II collagen immunostaining of the treated defects at 6 months after operation/treatment. (**A**) Low-power magnification of representative photomicrographs of the two treatment groups. The treatment with affinity-bound GF-loaded alginate hydrogel resulted in formation of a continuous cartilage layer. (**B**) High-power magnification of the defect and distant surrounding tissue in each treatment group. The treatment with affinity-bound GF-loaded alginate hydrogel resulted in similar stain intensity and pattern and morphological similarity to normal hyaline cartilage. In contrast, the treatment with empty hydrogel resulted in marked differences and reduction in stain intensity, mainly showing disorganised hypertrophic tissue and fibrocartilage. Bar = 200 μm. Dotted lines represent original defect borders.
GF = growth factor.

with the presence of major features of native hyaline cartilage, such as glossy macroscopic appearance, similar chondrocyte density and organisation and deposition of major cartilaginous ECM components, such as proteoglycans and type II collagen. Such effective cartilage reconstruction may be a result of several processes but mainly driven by an affinity-binding mechanism of GF presentation and its slow release. Initially, uncontrolled stem/progenitor cell migration is prevented by the presence of the dense hydrogel. This may promote cell condensation and contribute to their chondrogenic differentiation. Such process is suggested to be a primary mechanism of action for some hydrogels in clinical development [22]. Importantly, however, as judged by the inferior results seen in the defects treated with the empty hydrogel, only the presence of affinity-bound chondrogenic inducer TGFβ1 could direct the differentiation course into the formation of organised hyaline-like tissue. As a parallel process, alginate hydrogel is suggested to undergo slow dissolution by surface erosion, due to exchange of cross-linking calcium ions with sodium, allowing its gradual replacement by the regenerated tissue [23]. Intriguingly, the complete reconstruction

of the articular surface on top of an incomplete subchondral bone layer and the penetration of the regenerated cartilage into the bone region raise several possibilities of involvement of additional stem/progenitor cell populations in the regeneration process of the cartilage layer in addition to mesenchymal stem cells (MSCs) migrating from the bone marrow compartment. A particularly prominent source of regenerative cells may be the synovium and synovial fluid [24]. The synovium and cartilage originate from a common pool of progenitors during normal joint development [25]. Synovium-derived progenitors possess a robust chondrogenic potential that can contribute to endogenous repair [24]. Finally, migration and subsequent activation of resident chondrogenic stem/progenitor cells that may be present in healthy cartilage represent another interesting possibility [21]. The kinetics and relative contribution of various stem/progenitor cell sources to the regeneration of articular cartilage await further investigation.

The treatment with GF-affinity-bound bilayered hydrogel was associated with simultaneously augmented, although incomplete, subchondral bone regeneration. A hydrogel form of the applied biomaterial structurally resembles native ECM of the cartilage, with a dense polymer network with pore sizes in the submicron range [26]. However, these structural properties may be not optimal for osteoconduction and osteogenesis as it is generally recognised that scaffolds with pores of several hundreds of microns are more appropriate for bone regeneration [27]. Thus, such mismatch in physical properties of the applied material may have prevented realisation of the full potential of the affinity-bound osteogenic inducer, BMP-4. Of note, osteochondral defects represent only a minority of clinical cases, where the defects extend through the cartilage into the subchondral bone, while most defects (~80%) are confined to the cartilage layer [1].

The administration form of the cartilage repair product is an important component in the overall success of the treatment. Several strategies for articular cartilage repair focus on the development of solid implantable scaffolds [28]. Application of solid implants requires adaptation of the implant and/or the defect before final administration to maintain a good degree of integration with the surrounding tissue and sometimes is associated with the need for the significant extension of the defect depth to maintain implant stability [28]. Moreover, such administration may result in mismatch in the defect surface topography compared to its surroundings due to the solid nature of the implant. Insufficient integration and topographical mismatch subsequently may lead to biomechanical failure and tissue degeneration at the interface region [29]. The injectable alginate hydrogel is devoid of these disadvantages. The hydrogel represents an off-the-shelf solution that may be applied to any irregular defect without prior preparations. Moreover, the nature of the material allows its reshaping during application to match the specific structural needs, finally resulting in the formation of a shear-resistant and integrated layer with complete topographical matching to defect surroundings and opposing articulating surface. The GF-loaded affinity-binding alginate hydrogel represents a simple add-on approach to the MF procedure, which is a first-line treatment for articular cartilage defects [5]. Introducing the hydrogel application step after a MF operation, while only slightly extending the procedure duration, may result in a completely different and favourable functional outcome, due to the formation of high-quality articular cartilage. The injectable nature of the material permits its administration using established minimally invasive surgical techniques, such as arthroscopy.

Our study has several limitations. The treatment group size was small and did not allow the performance of additional biomechanical and biochemical (e.g., glycosaminoglycan (GAG)/DNA content) analyses. Also, the untreated group of animals was not included in the present study. Historical data strongly suggest that untreated osteochondral defects of similar size heal with predominantly fibrocartilaginous, and not hyaline, tissue, as expected [30]. These data allowed us to test the effect of biomaterials (with or w/o affinity-bound factors) on osteochondral regeneration and to reduce the number of the animals involved in the study. In addition, a longer follow-up (up to 1 year) would help to confirm a long-term efficacy and durability of the treatment, whereas interim noninvasive analyses, such as CT and compositional magnetic resonance imaging, may also be performed [31].

In conclusion, this proof-of-concept study shows that the treatment with acellular injectable GF-loaded affinity-binding alginate hydrogel results in effective restoration of articular cartilage with major hallmarks of hyaline tissue. These beneficial effects, attributed to spatial bio-inspired GF presentation, were shown in a clinically relevant large animal model after 6-month follow-up. The acellular and injectable nature of the biomaterial represents an effective off-the-shelf solution able to significantly augment current standard-of-care procedures, with strong translational potential and minimal implementation time, aiming at functional long-term relief in patients with articular cartilage damage.

Conflicts of interest

All contributing authors declare no conflicts of interest.

Acknowledgments

The study was supported by Kamin grant from the Ministry of Economy and Industry, Israel. We thank Jens Nellesen at Technical University (Dortmund, Germany) for the excellent technical assistance.

Appendix A. Supplementary data

Supplementary data related to this article can be found at https://doi.org/10.1016/j.jot.2018.08.003.

References

[1] Widuchowski W, Widuchowski J, Trzaska T. Articular cartilage defects: study of 25,124 knee arthroscopies. Knee 2007;14:177–82.

[2] Carbone A, Rodeo S. Review of current understanding of post-traumatic osteoarthritis resulting from sports injuries. J Orthop Res 2017;35:397–405.

[3] Huey DJ, Hu JC, Athanasiou KA. Unlike bone, cartilage regeneration remains elusive. Science 2012;338:917—21.
[4] Erggelet C, Vavken P. Microfracture for the treatment of cartilage defects in the knee joint - a golden standard? J Clin Orthop Trauma 2016;7:145—52.
[5] Makris EA, Gomoll AH, Malizos KN, Hu JC, Athanasiou KA. Repair and tissue engineering techniques for articular cartilage. Nat Rev Rheumatol 2015;11:21—34.
[6] Knutsen G, Drogset JO, Engebretsen L, Grontvedt T, Ludvigsen TC, Loken S, et al. A randomized multicenter trial comparing autologous chondrocyte implantation with microfracture: long-term follow-up at 14 to 15 years. J Bone Joint Surg Am 2016;98:1332—9.
[7] Freeman I, Kedem A, Cohen S. The effect of sulfation of alginate hydrogels on the specific binding and controlled release of heparin-binding proteins. Biomaterials 2008;29:3260—8.
[8] Ruvinov E, Freeman I, Fredo R, Cohen S. Spontaneous coassembly of biologically active nanoparticles via affinity binding of heparin-binding proteins to alginate-sulfate. Nano Lett 2016;16:883—8.
[9] Ruvinov E, Leor J, Cohen S. The promotion of myocardial repair by the sequential delivery of IGF-1 and HGF from an injectable alginate biomaterial in a model of acute myocardial infarction. Biomaterials 2011;32:565—78.
[10] Ruvinov E, Leor J, Cohen S. The effects of controlled HGF delivery from an affinity-binding alginate biomaterial on angiogenesis and blood perfusion in a hindlimb ischemia model. Biomaterials 2010;31:4573—82.
[11] Grulova I, Slovinska L, Blasko J, Devaux S, Wisztorski M, Salzet M, et al. Delivery of alginate scaffold releasing two trophic factors for spinal cord injury repair. Sci Rep 2015;5:13702.
[12] Re'em T, Witte F, Willbold E, Ruvinov E, Cohen S. Simultaneous regeneration of articular cartilage and subchondral bone induced by spatially presented TGF-beta and BMP-4 in a bilayer affinity binding system. Acta Biomater 2012;8:3283—93.
[13] ASTM F2451 — 05. Standard guide for in vivo assessment of implantable devices intended to repair or regenerate articular cartilage. Am Soc Test Mater Int 2010.
[14] Guidance for Industry. Preparation of IDEs and INDs for products intended to repair or replace knee cartilage. US Food Drug Adm 2011.
[15] van Gaalen SM, Kruyt MC, Geuze RE, de Bruijn JD, Alblas J, Dhert WJA. Use of fluorochrome labels in in vivo bone tissue engineering research. Tissue Eng B Rev 2009;16:209—17.
[16] Jagodzinski M, Liu C, Guenther D, Burssens A, Petri M, Abedian R, et al. Bone marrow-derived cell concentrates have limited effects on osteochondral reconstructions in the mini pig. Tissue Eng C Meth 2013;20:215—26.
[17] van den Borne MP, Raijmakers NJ, Vanlauwe J, Victor J, de Jong SN, Bellemans J, et al. International cartilage repair S. International cartilage repair society (ICRS) and Oswestry macroscopic cartilage evaluation scores validated for use in autologous chondrocyte implantation (ACI) and microfracture. Osteoarthritis Cartilage 2007;15:1397—402.
[18] Janning C, Willbold E, Vogt C, Nellesen J, Meyer-Lindenberg A, Windhagen H, et al. Magnesium hydroxide temporarily enhancing osteoblast activity and decreasing the osteoclast number in peri-implant bone remodelling. Acta Biomater 2010;6:1861—8.
[19] Niederauer GG, Slivka MA, Leatherbury NC, Korvick DL, Harroff HH, Ehler WC, et al. Evaluation of multiphase implants for repair of focal osteochondral defects in goats. Biomaterials 2000;21:2561—74.
[20] Stolz M, Gottardi R, Raiteri R, Miot S, Martin I, Imer R, et al. Early detection of aging cartilage and osteoarthritis in mice and patient samples using atomic force microscopy. Nat Nanotechnol 2009;4:186—92.
[21] Wang M, Yuan Z, Ma N, Hao C, Guo W, Zou G, et al. Advances and prospects in stem cells for cartilage regeneration. Stem Cell Int 2017;2017:4130607.
[22] Goldshmid R, Cohen S, Shachaf Y, Kupershmit I, Sarig-Nadir O, Seliktar D, et al. Steric interference of adhesion supports in-vitro chondrogenesis of mesenchymal stem cells on hydrogels for cartilage repair. Sci Rep 2015;5:12607.
[23] Ruvinov E, Cohen S. Alginate biomaterial for the treatment of myocardial infarction: progress, translational strategies, and clinical outlook: from ocean algae to patient bedside. Adv Drug Deliv Rev 2016;96:54—76.
[24] Jones BA, Pei M. Synovium-derived stem cells: a tissue-specific stem cell for cartilage engineering and regeneration. Tissue Eng Part B Rev 2012;18:301—11.
[25] Archer CW, Dowthwaite GP, Francis-West P. Development of synovial joints. Birth Defects Res C Embryo Today 2003;69:144—55.
[26] Vega SL, Kwon MY, Burdick JA. Recent advances in hydrogels for cartilage tissue engineering. Eur Cell Mater 2017;33:59—75.
[27] Tang D, Tare RS, Yang LY, Williams DF, Ou KL, Oreffo RO. Biofabrication of bone tissue: approaches, challenges and translation for bone regeneration. Biomaterials 2016;83:363—82.
[28] Kon E, Robinson D, Verdonk P, Drobnic M, Patrascu JM, Dulic O, et al. A novel aragonite-based scaffold for osteochondral regeneration: early experience on human implants and technical developments. Injury 2016;47(Suppl 6):S27—32.
[29] Ahsan T, Sah RL. Biomechanics of integrative cartilage repair. Osteoarthritis Cartilage 1999;7:29—40.
[30] Harman BD, Weeden SH, Lichota DK, Brindley GW. Osteochondral autograft transplantation in the porcine knee. Am J Sports Med 2006;34:913—8.
[31] Lakin BA, Snyder BD, Grinstaff MW. Assessing cartilage biomechanical properties: techniques for evaluating the functional performance of cartilage in Health and disease. Annu Rev Biomed Eng 2017;19:27—55.